Acta Biochim Biophys Sin 2026, 58(10): 2384–2388
https://cstr.cn/32197.14.abbs.2026066
https://doi.org/10.3724/abbs.2026066
New Phenomenon

New Phenomenon

FGF10 is essential for postnatal meibomian gland development in mice

Zelong Jiang[1,3,4,†], Lue Xiang[5,†], Yubin Yu[6,†], Qiqi Wu[1,3,4], Shuangyan Peng[1,3,4], Yang Yu[1,3,4], Fangyi Lv[1,3,4], Zi Jin[1,3,4], Deyin He[1,3,4], Juan Li[1,3,4], Xiaokun Li[1,3,4], Xiaojie Wang[1,3,4,*], and Fengqin Rao[1,2,3,4,*]

[1]School of Pharmaceutical Sciences, Wenzhou Medical University, Wenzhou 325035, China, [2]College of Nursing, Wenzhou Medical University, Wenzhou 325035, China, [3]Laboratory of Zhejiang Province for Pharmaceutical Engineering and Development of Growth Factors, Collaborative Biomedical Innovation Center of Wenzhou, Wenzhou 325035, China, [4]Research Units of Clinical Translation of Cell Growth Factors and Diseases, Chinese Academy of Medical Science, Beijing 100021, China, [5]State Key Laboratory of Ophthalmology, Optometry, and Vision Science, Eye Hospital, Wenzhou Medical University, Wenzhou 325027, China, and [6]Department of Ophthalmology, The Second Affiliated Hospital and Yuying Children's Hospital of Wenzhou Medical University, Wenzhou 325002, China

[†]These authors contributed equally to this work.

*Correspondence address. E-mail: rfqwzmc@foxmail.com (F.R.); wangxiaojie1972@126.com (X.W.)

Received 28 December 2025 Accepted 25 March 2026 Published 19 May 2026

The important role of fibroblast growth factor 10 (FGF10) in the ocular surface has attracted substantial attention from researchers over the past two decades [1–3]. Its receptor, FGFR2, maintains meibomian gland (MG) homeostasis by regulating Krt5$^+$ basal progenitors in the adult stage, and the deletion of *Fgfr2* causes aberrant meibocyte differentiation, leading to ductal hyper-stratification, luminal occlusion, and secondary acinar atrophy due to impaired meibocyte renewal. However, the detailed function of FGF10 in the early development of MG remains largely unknown.

To systematically assess the impact of FGF10 on the ocular surface, our group generated an *Fgf10* mutant mouse model with the removal of its entire exon two, leading to loss of function of *Fgf10* in mice (Figure 1A). Adult *Fgf10*$^{+/-}$ mice exhibited lacrimal gland agenesis and possessed smaller Harderian glands than their wild-type littermates (Supplementary Figure S1A). We also evaluated tear production and corneal integrity. *Fgf10*$^{+/-}$ mice displayed a marked increase in corneal fluorescein staining and significantly reduced tear volume, indicative of epithelial damage (Supplementary Figure S1B,C). The body weights of *Fgf10*$^{+/-}$ mice were comparable to those of wild-type controls (Supplementary Figure S1D). Histological analysis further revealed that while the Harderian gland alveoli in wild-type mice were lined by a single epithelial layer, those in *Fgf10*$^{+/-}$ mice displayed a multilayered, hyperplastic epithelium (Supplementary Figure S1E). The loss of function of *Fgf10* has been previously reported to lead to lacrimal gland development failure and atrophy of the Harderian gland. Interestingly, we also observed MG atrophy in *Fgf10*$^{+/-}$ mice (Figure 1B). To obtain detailed information and an overview of the developmental defects of the MG in *Fgf10*-deficient mice, we performed time-series Oil Red O staining. At P14 and P21, we could clearly see shorter, thinner, and disordered MG in *Fgf10*$^{+/-}$ mice, indicating that the proliferation and differentiation of the acinar cells were severely affected. This phenomenon was not alleviated in *Fgf10*$^{+/-}$ mice at P135, indicating an unrecoverable and pathogenic developmental process (Figure 1C–E). The cryosection samples confirmed the acini showing lower signals (reduced lipid production) or displaying smaller acini in *Fgf10*$^{+/-}$ mice (Figure 1F). Collectively, these findings establish that haploinsufficiency of *Fgf10* leads to severe glandular malformations, impaired tear production, and compromised corneal epithelial integrity.

To elucidate the molecular mechanisms underlying the observed developmental defects, we performed RNA sequencing (RNA-Seq) on MGs isolated from wild-type and *Fgf10*$^{+/-}$ mice at P14 and P21. Three groups of mice were used, with each group consisting of three wild-type and three knockout mice. Heatmap analysis indicated that the expression levels of macrophage-related genes showed significant changes in the *Fgf10*$^{+/-}$ mice at P14 (Figure 2A, Supplementary Figure S3A). Gene Ontology (GO) enrichment analysis of the differentially expressed genes (DEGs) identified that the immune-related signature was further pronounced, with top-ranking enriched processes including antigen processing and presentation (GO:0002606: positive regulation of dendritic cell antigen processing and presentation; GO:0019886: antigen processing and presentation of exogenous peptide antigen via MHC class II), as well as pathways associated with macrophages (GO:0010759: positive regulation of macrophage chemotaxis) at P21 (Figure 2B, Supplementary Figure S3B). Taken together, these transcriptomic analyses demonstrate that *Fgf10* deficiency in the developing MG

© The Author(s) 2026. This is an open access article distributed under the terms of the Creative Commons Attribution Non-Commercial License (https://creativecommons.org/licenses/by-nc/4.0/).

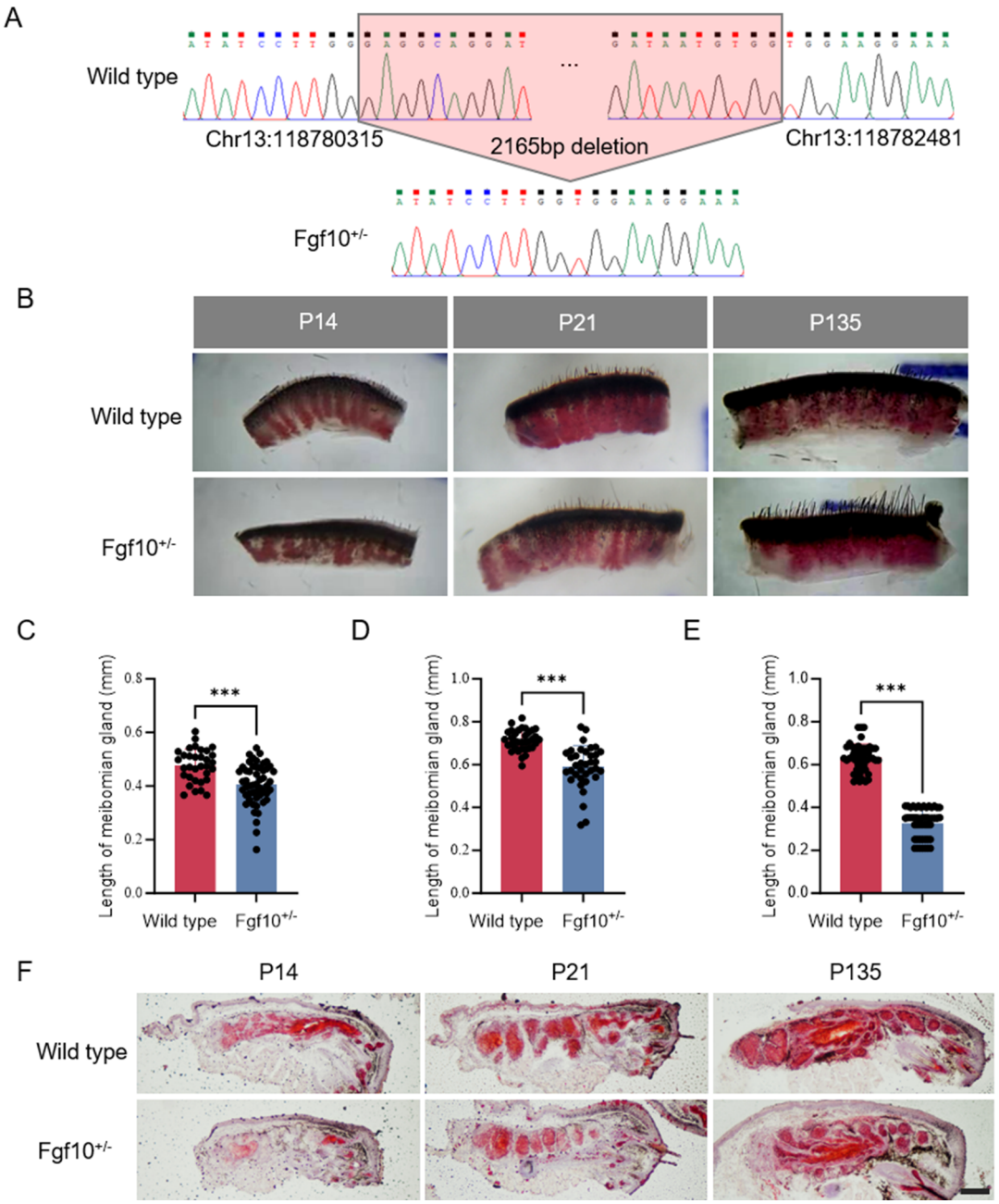


Figure 1. Knockout strategy and genotyping of *Fgf10*$^{+/-}$ mice and phenotypic changes in the MG (A) Depletion of exon two of *Fgf*10. A 2165 bp sequence was removed from the genome of *Fgf10*$^{+/-}$ mice. (B) Representative images of Oil Red O staining of MGs from wild-type and *Fgf10*$^{+/-}$ mouse upper eyelids at P14, P21, and P135. (C–E) Measurements of MG length at (C) P14, (D) P21, and (E) P135. (F) Oil Red O staining of mouse MG cryosections during development. Representative images of Oil Red O staining of MGs from wild-type and *Fgf10*$^{+/-}$ mouse upper eyelids at P14, P21, and P135. Scale bar: 1 mm. These results are consistent with the observations using whole tissue staining. $n = 6$. Normalized values represent the mean ± SD. $^{***}P < 0.001$. Student's *t* test.

leads to a profound dysregulation of immune-related molecular pathways.

Given that our transcriptomic analysis pointed to a dysregulation of macrophage and dendritic cell-related pathways, we next sought to investigate these myeloid cell populations *in situ*. To visualize these cells, we crossed *Fgf10*$^{+/-}$ mice with *Cx3cr1*$^{GFP/+}$ reporter mice, in which resident macrophages and a subset of dendritic cells are labeled with GFP. At P21, we observed a distinct population of CX3CR1$^{GFP/+}$ cells localized within the inter-acinar stroma of wild-type (WT) MGs (Supplementary Figure S2A). In stark contrast, the number of these CX3CR1$^{GFP/+}$ cells was significantly reduced in the MGs of *Fgf10*$^{+/-}$ mice (Supplementary Figure S2B).

Since FGF10 targets meibomian immune cells, if this cell factor impacts the development of the MG through immune cells, the direct disruption of these cells should give rise to similar developmental defects. CSF1R is a cell membrane receptor in some

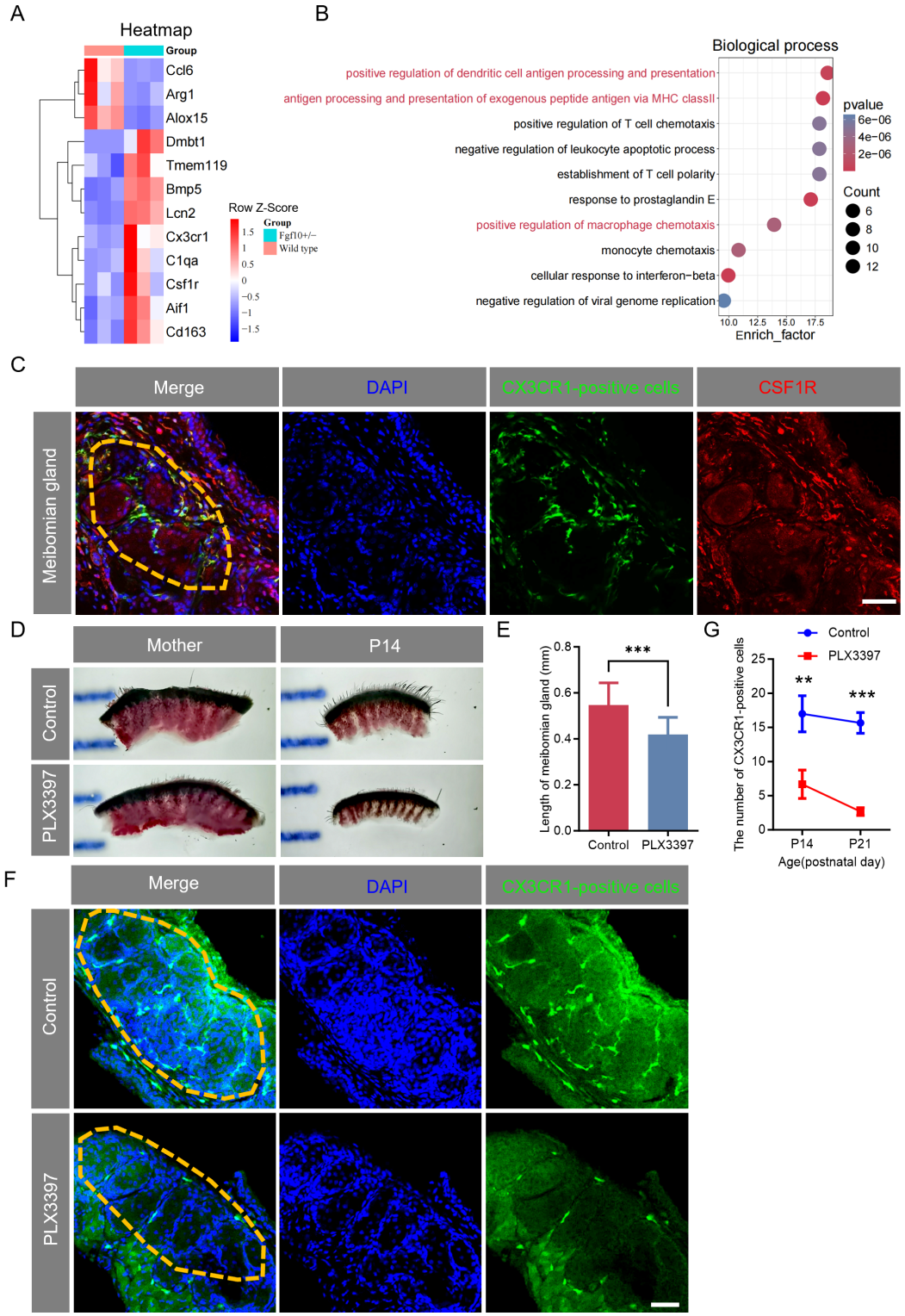


Figure 2. Transcriptome analyses and pharmacological ablation of CX3CR1-positive cells in the mouse MG in the early developmental stage (A) Heatmap showing significant changes in the expression levels of macrophage-related genes in *Fgf10*$^{+/-}$ mice compared to wild-type mice. (B) Biological process analysis. The red-blue gradient color bar shows the *P* values of BP items. Red GO denotes macrophage-related BPs. (C) Immunostaining of CSF1R in the MG of CX3CR1$^{GFP/+}$ mice. Scale bar: 50 μm. (D) The morphology of the MG is not changed in the mother; however, shorter and slenderer glands are observed in the pups at P14. (E) Statistical analysis of the MG length at P14. (F) Histology results reveal the ablation of CX3CR1-positive cells in the mouse MGs. The orange dotted areas are the locations of acini. Scale bar: 50 μm. (G) Relative number of CX3CR1-positive cells in the region of acini in panel (F). The normalized values represent the mean ± SD. $^{**}P < 0.01$ and $^{***}P < 0.001$. Student's *t* test.

immune cells, and it is expressed in myeloid immune cells, such as monocytes and macrophages. Immunofluorescence staining showed that almost every CX3CR1-positive cell expressed CSF1R (Figure 2C). The pharmacological application of PLX3397 is widely used to ablate this type of immune cell in tissues. The *Cx3cr1*$^{GFP/+}$ mice were randomly classified into two groups: a control group and an experimental group. The experimental group was induced by intraperitoneal injection of PLX3397 (40 mg/kg) twice a day into lactating females from P4 to P14, and the control group was administered the same volume of vehicle. Interestingly, the offspring that received PLX3397 exhibited shorter and thinner MGs by Oil Red O staining at P14, partially reflecting morphological changes in *Fgf10*$^{+/-}$ mice (Figure 2D,E). This treatment regimen effectively reduced the number of Cx3cr1-positive cells within the MGs at both P14 and P21, confirming successful cell depletion (Figure 2F,G). Importantly, the body weights of PLX3397-treated pups were comparable to those of vehicle-treated controls at both time points. These results demonstrate that CSF1R-dependent myeloid cells are required for proper MG morphogenesis during early postnatal development.

FGF10 functions as a canonical paracrine signaling molecule secreted by mesenchymal cells to activate its primary epithelial receptor, FGFR2. Moreover, FGFR2 is recognized as an essential factor driving progenitor differentiation into mature acinar cells in the MG. Conditional deletion of *Fgfr2* leads to ductal occlusion, acinar atrophy, and impaired meibocyte differentiation in the adult stage [4–6]. In our *Fgf10*$^{+/-}$ mouse model, we found that FGF10 is essential for MG morphogenesis in the early developmental stage. Notably, the associated immune dysregulation, particularly the altered distribution of CX3CR1-positive cells upon *Fgf10* ablation, implicates macrophages as key mediators of FGF10 signaling during development (Figure 2). This introduces a novel immunomodulatory axis in MG organogenesis, extending beyond the established epithelial-autonomous role of FGFR2 in adult homeostasis.

A central finding of our study is that resident immune cells represent a key mechanistic link between FGF10 signaling and proper MG organogenesis. It is possible that CX3CR1-positive cells within this niche serve as stromal architects, providing trophic support for epithelial progenitor proliferation, or as regulators of ductal patterning to ensure proper luminal formation during morphogenesis. Defining the precise crosstalk between FGF10 and these immune populations will be a critical next step in understanding MG development and potentially treating MG dysfunctions.

Our previous pharmacological studies have demonstrated the pleiotropic effects of topical recombinant FGF10. In a rabbit model of corneal injury, the drug not only accelerated epithelial wound healing but also exhibited significant anti-inflammatory and anti-neovascularization properties [7]. Given that corneal epithelial compromise is a central event in the pathogenesis of dry eye disease, these findings positioned FGF10 as a promising therapeutic agent. This notion is further supported by studies demonstrating its capacity to maintain corneal epithelial integrity and tear film stability through diverse mechanisms, including suppressing inflammation through the HMGB1/TLR4 axis [8].

The present study fundamentally advances this understanding by providing a critical etiological link. While prior work focused on the restorative capacity of exogenous FGF10, our genetic loss-of-function model reveals the indispensable role of endogenous FGF10 in the proper development and structural maintenance of the MGs. In summary, we establish a critical role for FGF10 in the postnatal organogenesis of the MG. These findings also lay the groundwork for exploring therapeutic interventions. Developing a new protein delivery system [9,10] of FGF10 directly to the MG acini may offer a promising approach for the treatment of MGD (MG dysfunction). Animal care followed the ARVO Statement for the Use of Animals in Ophthalmic and Vision Research, and with the approval of the Animal Ethical Committee of Wenzhou Medical University (No. WYDW20200539).

Supplementary Data

Supplementary data are available at *Acta Biochimica et Biophysica Sinica* online.

Data Availability

The RNA-seq data was accessible in the SRA database with the accession number of SRR24751673, SRR24751674, SRR24751675, SRR24751676, SRR24751677, SRR24751678, SRR24751679, SRR24751680, SRR24751681, SRR24751682, SRR24751683, and SRR24751684.

Author Contributions

Z.L. Jiang: data acquisition, data analysis, visualization, writing – original draft; L. Xiang: data acquisition, data analysis, visualization, writing – original draft; Y.B. Yu: visualization, writing – original draft; Q.Q. Wu: data curation, visualization; S.Y. Peng: data curation, data analysis; Y. Yu: data curation, data analysis; F. Y. Lv: visualization; Z. Jin: visualization; D.Y. He: data analysis; J. Li: data analysis; X.K. Li: conceptualization, funding acquisition; X. J. Wang: conceptualization, writing – review & editing, funding acquisition; F.Q. Rao: conceptualization, data acquisition, writing – review & editing. All authors read and approved the final manuscript.

Funding

This work was supported by the grants from the Key Research and Development Projects of Zhejiang Province (No. 2022C03110), the National Natural Science Foundation of China (No. 81971843), the State Project for Essential Drug Research and Development (No. 2016ZX09101117), the Natural Science Foundation of Zhejiang Province (No. LY17H150002), the CAMS Innovation Fund for Medical Sciences (No. 2019-I2M-5-028), the Wenzhou Science and Technology Bureau (Nos. ZY2020024 and Y20190050), and the Wenzhou Innovation Team (Growth Factor Drug Development, No. 201801).

Conflict of Interest

The authors declare that they have no conflict of interest.

References

1. Wang Q, Tao C, Wu Y, Anderson KE, Makrides N, Hannan A, Peregrin J, *et al.* FGF-induced phospholipase Cγ signaling regulates lacrimal gland branching by competing with PI3K in phosphoinositide metabolism. *Cell Rep* 2025, 44: 116046
2. Makrides N, Wang Q, Tao C, Schwartz S, Zhang X. Jack of all trades, master of each: the diversity of fibroblast growth factor signalling in eye development. *Open Biol* 2022, 12: 210265
3. Finburgh EN, Mauduit O, Noguchi T, Bu JJ, Abbas AA, Hakim DF,

Bellusci S, *et al.* Role of FGF10/FGFR2b signaling in homeostasis and regeneration of adult lacrimal gland and corneal epithelium proliferation. *Invest Ophthalmol Vis Sci* 2023, 64: 21

4. Yang X, Reneker LW, Zhong X, Huang AJW, Jester JV. Meibomian gland stem/progenitor cells: the hunt for gland renewal. *Ocular Surf* 2023, 29: 497–507
5. Yang X, Zhong X, Lin H, Huang AJW, Reneker LW. Deletion of *Fgfr2* in ductal basal epithelium with tamoxifen induces obstructive meibomian gland dysfunction. *Invest Ophthalmol Vis Sci* 2024, 65: 36
6. Reneker LW, Wang L, Irlmeier RT, Huang AJW. Fibroblast growth factor receptor 2 (FGFR2) is required for meibomian gland homeostasis in the adult mouse. *Invest Ophthalmol Vis Sci* 2017, 58: 2638–2646
7. Wang X, Zhou X, Ma J, Tian H, Jiao Y, Zhang R, Huang Z, *et al.* Effects of keratinocyte growth factor-2 on corneal epithelial wound healing in a rabbit model of carbon dioxide laser injury. *Biol Pharm Bull* 2010, 33: 971–976
8. Wang Y, Xu Z, Wei L, Lu Y, Shi Y, Wen S, Lv X, *et al.* KGF-2 alleviates dry eye disease by regulating the HMGB1/TLR4 pathway. *Invest Ophthalmol Vis Sci* 2025, 66: 28
9. Li S, Lu Z, Huang Y, Wang Y, Jin Q, Shentu X, Ye J, *et al.* Anti-oxidative and anti-inflammatory micelles: break the dry eye vicious cycle. *Adv Sci* 2022, 9: e2200435
10. Zhang Y, Zhou T, Wang K, Luo C, Chen D, Lv Z, Han H, *et al.* Corneal mucin-targeting liposome nanoplatforms enable effective treatment of dry eye diseases by integrated regulation of ferroptosis and inflammation. *Adv Sci* 2025, 12: e2411172